# Comments on "Tropical Convection and the Energy Balance at the Top of the Atmosphere"

MING-DAH CHOU

*NASA Goddard Space Flight Center, Laboratory for Atmospheres, Greenbelt, Maryland*

RICHARD S. LINDZEN

*Department of Earth, Atmospheric, and Planetary Sciences, Massachusetts Institute of Technology, Cambridge, Massachusetts*

14 February 2002 and 26 March 2002

Analyses of the Earth Radiation Budget Experiment (ERBE; Barkstrom 1984) data show that the shortwave (SW) and longwave (LW) cloud radiative forcing (CRF) at the top of the atmosphere (TOA) in the tropical deep convective regions have a similar magnitude but opposite signs. The CRF is defined as the difference between the full-sky and clear-sky radiative fluxes. Hartmann et al. (2001, hereafter HMF) computed the CRF for individual cloud types using a radiative transfer model with the cloud information taken from the International Satellite Cloud Climate Project (ISCCP; Rossow and Schiffer 1991) data archive. They found that individually each cloud type had a large impact on the radiation at the TOA, but collectively the effect was small. From the analyses of the ERBE data, they claimed that the net CRF at the TOA is small not only over deep convective regions but also over the nonconvective regions. The perceived small CRF led them to conclude that the contrast in the net TOA radiation between the convective and nonconvective regions must also be small. HMF used a simple model to investigate the relation between convection and radiation in the Tropics. They hypothesized that the small contrast in the TOA radiation between the convective and nonconvective regions was due to the high sensitivity of circulation to the sea surface temperature (SST) gradient and the high sensitivity of cloud albedo to vertical velocity.

However, the ERBE data do not generally show a small contrast in the TOA radiation between the convective and nonconvective regions, and the model used by HMF, therefore, seems unlikely to represent the real physical processes involving convection, radiation, and climate in an appropriate way.

Figure 1a shows the net radiation and CRF in the Pacific averaged over five years (1985–89) for the equatorial band 10°S–10°N derived from the ERBE data. The net heating of the earth–atmosphere system attains a maximum value of ~80 W $m^{-2}$ west of 160°E and decreases continuously eastward to a value of ~50 W $m^{-2}$ at 260°E. The longitudinal distribution of the CRF (Fig. 1b) is very similar to that of the net radiation. The CRF ranges from −5 W $m^{-2}$ west of the date line to −32 W $m^{-2}$ at 260°E. The contrast between the deep convective region west of 160°E and the suppressed region to the east is 1:1.6 for the net radiation and 1:6 for the CRF. These contrasts can hardly be considered as small. Averaged over the 5 ERBE years (1985–89), the full-sky net TOA radiation in the Tropics (30°S–30°N) is 48.6 W $m^{-2}$, the clear-sky net radiation is 61.1 W $m^{-2}$, and the CRF is −12.5 W $m^{-2}$. Thus, the CRF in the Tropics as a whole is significant.

HMF suggested that the small CRF in the deep convective region as found by Kiehl (1994) is not a coincidence but is a combined effect of an ensemble of various types of clouds occurring at various heights and with a large range of optical thickness. They further suggested that the small CRF is a result of the feedback between convection, cloud albedo, and the SST gradient. In fact, the small CRF in the deep convective region is easy to explain. Clouds have the effects of reflecting SW radiation and reducing OLR. Except for thin clouds at high altitudes, the SW CRF in the Tropics is greater than the LW CRF. That the net CRF at 260°E is large, approximately −30 W $m^{-2}$, can be seen in Fig. 1b. This region is in the descending branch of the Walker circulation where the deep convection is suppressed and the boundary layer clouds are extensive. For those

*Corresponding author address:* Dr. Ming-Dah Chou, NASA Goddard Space Flight Center, Code 913, Greenbelt, MD 20771.
E-mail: chou@climate.gsfc.nasa.gov

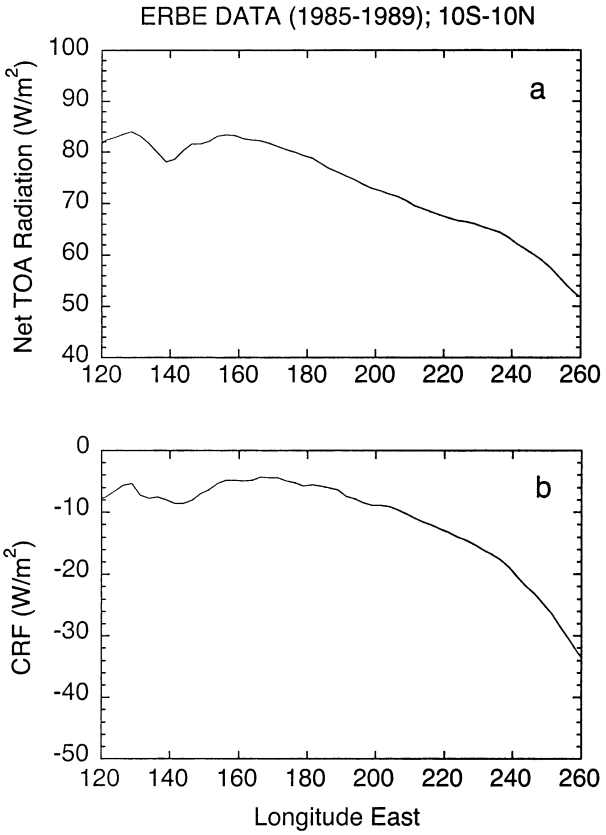


FIG. 1. Longitudinal distributions of (a) the net radiation and (b) cloud radiative forcing in the equatorial Pacific (10°S–10°N) averaged over 5 yr (1985–89). The radiative fluxes are taken from the ERBE data archive.

boundary layer clouds, the contrast between the cloud-top temperature and the SST is small, and so is the LW CRF. On the other hand, those clouds are highly reflective to SW radiation, and the SW CRF is large. The result is a large negative CRF. Westward from 260°E, the boundary layer depth and, hence, the cloud height increase, but the cloud cover decreases. The increase in cloud height enhances the difference between the cloud temperature and the SST, which leads to an enhanced LW CRF. Thus, the net CRF decreases westward toward the date line. West of the date line is the deep convective region, where high-level clouds are extensive. The CRF is small, within $-10$ W m$^{-2}$.

In the simple model of HMF, the Tropics are divided into a convective region and a nonconvective region. Each of these two regions is characterized by the SST, $T$; the net radiation at TOA, $R$; and the areal extent, $A$. The rate of change of the SST is given in their model by

$$c\frac{dT_1}{dt} = R_1 - \frac{M}{A_1}c_p(\theta_{e1} - \theta_{e2}) + \mathrm{Exp}_1 \qquad (1)$$

$$c\frac{dT_2}{dt} = R_2 + \frac{M}{A_2}c_p(\theta_{e1} - \theta_{e2}) + \mathrm{Exp}_2, \qquad (2)$$

where $c$ is the heat capacity of the ocean mixed layer, $M$ is the mass flux between the two regions, $c_p$ is the heat capacity of air, $\theta_e$ is the saturation potential temperature of the surface air, Exp is the export of heat out of the domain of interest, and the subscripts 1 and 2 denote the convective and nonconvective regions, respectively.

Assuming that exports of heat out of the convective and nonconvective regions are the same, equilibrium solutions for $T_1$, $T_2$, $R_1$, and $R_2$ are obtained by time integration of Eqs. (1) and (2), so that

$$R_1 - R_2 = Mc_p(\theta_{e1} - \theta_{e2})\left(\frac{1}{A_1} + \frac{1}{A_2}\right). \qquad (3)$$

Thus, the imbalance between $R_1$ and $R_2$ equals the transport of heat from the convective region to the nonconvective region.

The mass flux between the two regions, which is related to the vertical pressure velocity $\omega$, is given by

$$M = A_2\frac{\omega_2}{g} = -A_1\frac{\omega_1}{g}, \qquad (4)$$

where $g$ is the gravitational acceleration. The convective area fraction $A_1$ is set to be 0.3. The vertical pressure velocity in the convective region is assumed to be linearly proportional to the temperature contrast between the convective and nonconvective regions,

$$\omega_1 = -\gamma(T_1 - T_2) = -\gamma\Delta T, \qquad (5)$$

where $\gamma$ is a disposable constant.

The net radiation at TOA is given by

$$R_i = S(1 - \alpha_i) - F_i, \qquad (6)$$

where $S$ is the insolation at TOA, $\alpha$ is the albedo, $F$ is the OLR, and $i = 1$ or 2. The OLR in each region is assumed to vary only slightly with the SST and is practically fixed at 190 and 280 W m$^{-2}$ in the convective and nonconvective regions, respectively. The albedo in the nonconvective region $\alpha_2$ is fixed at 0.1, and the albedo in the convective region is assumed to be a function of vertical pressure velocity and SST,

$$\alpha_1 = \alpha_2 - \lambda\omega_1 q^*(T_1), \qquad (7)$$

where $\lambda$ is a disposable constant, and $q$ is the saturation water vapor mixing ratio.

Equation (5) has the convection and, hence, atmospheric overturning increasing with increasing temperature contrast between the two regions. Equation (7) has the cloud albedo in the convective region increasing with increasing convection for a positive $\lambda$. As $\alpha_1$ increases with increasing $T_1$, the net radiation $R_1$ will decrease, which will then lead to a decrease in both $T_1$ and the temperature contrast between the two regions. The decrease in the temperature contrast will cause weaker convection, which, according to Eq. (7), will reduce the albedo $\alpha_1$ for a positive $\lambda$. Thus, it constitutes a negative feedback loop between SST, convection,

cloud albedo, and radiation. The strength of the feedback is dependent upon the values of $\gamma$ and $\lambda$.

From Eq. (7), we have

$$\lambda = -\frac{1}{q^*(T_1)}\frac{\Delta\alpha_1}{\Delta\omega_1}. \tag{8}$$

To estimate the albedo sensitivity parameter $\lambda$, HMF derived values of $\Delta\alpha_1$ and $\Delta\omega_1$ by taking the albedo difference and the vertical velocity difference between the convective and nonconvective regions,

$$\Delta\alpha_1 = \alpha_1 - \alpha_2 \tag{9}$$

$$\Delta\omega_1 = \omega_1 - \omega_2, \tag{10}$$

so that

$$\lambda = -\frac{1}{q^*(T_1)}\left(\frac{\alpha_1 - \alpha_2}{\omega_1 - \omega_2}\right). \tag{11}$$

By assuming an albedo contrast of 0.25 between the convective and nonconvective regions, they found

$$\frac{\alpha_1 - \alpha_2}{\omega_1 - \omega_2} = -1.25 \times 10^2 \quad (\text{Pa s}^{-1})^{-1} \tag{12}$$

and $\lambda = 5 \times 10^3$ (Pa s$^{-1}$)$^{-1}$ for $q^* = 0.02$. Thus, $\lambda$ has a positive value, and the albedo in the convective region increases as convection strengthens.

Since, as applied by HMF, $\Delta\alpha_1$ and $\Delta\omega_1$ are the changes in albedo and vertical velocity of the convective region between either two different climate states or two different times, Eqs. (9) and (10) are of course incorrect. Instead, the correct representations should be

$$\Delta\alpha_1 = \alpha_1^{\text{a}} - \alpha_1^{\text{b}} \tag{13}$$

$$\Delta\omega_1 = \omega_1^{\text{a}} - \omega_1^{\text{b}} \tag{14}$$

where the superscripts a and b denote two different climate states. Therefore, the sensitivity of albedo to the vertical velocity estimated by HMF based on the differences between the convective and nonconvective regions is unrelated to the sensitivity given in Eq. (8). Equation (8) considers only the albedo and vertical velocity in the convective region. There is no evidence that the albedo in the convective region increases with increasing vertical velocity as HMF claimed.

From Eqs. (5) and (7), HMF estimated the sensitivity of albedo to SST from

$$\frac{\Delta\alpha}{\Delta T} = \lambda\gamma q^*. \tag{15}$$

Based on the results of Ramanathan and Collins (1991) on the relation between the interannual variations of the SST and the absorption of solar radiation, HMF estimated that

$$\frac{\Delta\alpha}{\Delta T} = 0.04 \text{ K}^{-1} \tag{16}$$

and $\lambda\gamma \approx 2$ for $q^* = 0.02$. They found that for $\lambda\gamma \approx 2$ the model predicted a strong feedback that brought the net radiation in the convective region close to that in the nonconvective region.

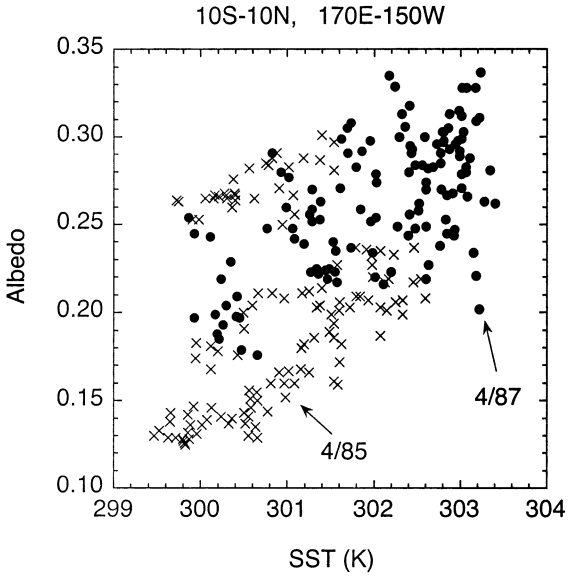


FIG. 2. A scatterplot relating albedo to SST in the central equatorial Pacific (10°S–10°N, 170°E–150°W) during Apr 1985 and Apr 1987. Each point represents monthly mean albedo from ERBE archive and SST from the NCEP analysis. The spatial resolution for each point is 2.5° × 2.5° lat–lon.

There are problems with this analysis of the albedo sensitivity to SST. First, Eq. (15) is not correct. From Eqs. (5) and (7), the albedo sensitivity should be

$$\frac{\Delta\alpha_1}{\Delta(T_1 - T_2)} = \lambda\gamma q^* \tag{17}$$

so that the albedo in the convective region changes with the temperature contrast between the convective and nonconvective regions.

Second, the sensitivity of albedo to SST cannot be derived by comparing the data associated with interannual variations. To demonstrate this point, we show in Fig. 2 a scatterplot that relates albedo to SST in the central equatorial Pacific (10°S–10°N, 170°E–150°W) during April 1985 and April 1987. These two months are the same as that used in Ramanathan and Collins (1991). Each point represents monthly mean albedo from the ERBE data archive and SST from the National Centers for Environmental Prediction (NCEP) analysis (Reynolds and Smith 1994). The spatial resolution for each point is 2.5° × 2.5° latitude–longitude. The year 1987 is an El Niño, and the SST in the central and eastern equatorial Pacific was abnormally high. Figure 3 shows the longitudinal distribution of equatorial SST of these two months. Compared to April 1985, the SST in the central and eastern equatorial Pacific increased significantly by 1.0–1.4°C in April 1987, but the warm pool region (140°–160°E) cooled slightly by ~0.2°C. Correspondingly, the center of deep convection shifted

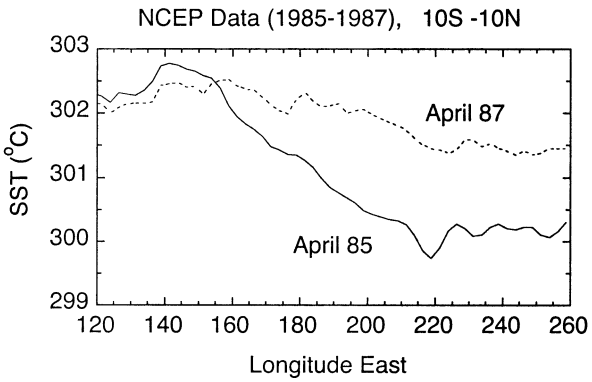


FIG. 3. Longitudinal distribution of SST in the equatorial Pacific (10°S–10°N) for Apr 1985 and Apr 1987. The SST is taken from the NCEP analysis.

eastward by ~50° longitude from the Maritime Continent to the central equatorial Pacific (Chou 1994). Associated with the eastward shift of the deep convection, Fig. 2 shows that both albedo and SST in the central equatorial Pacific are larger in April 1987 than in April 1985. These changes are unrelated to the sensitivity given in Eq. (17) and are irrelevant to the model of HMF. In fact, the central equatorial Pacific was in the descending domain of the Walker circulation during April 1985 but was in the ascending domain during April 1987. The albedo difference between these two months is equivalent to the incorrect equation (9) but not equivalent to the correct equation (13).

Strong updrafts in the convection cores constitute only a small fraction of the Tropics. Most of the Tropics are in the regions where the air is descending. Even the detrained thick anvil clouds are in the regions of descending motion. The simple model of HMF assigns a fractional area of 0.3 to the convective region. With this large extent of the convective region, it must include both the deep convection cores and the extended anvil and cirrus clouds, both optically thick and thin. It is not clear what the albedo of the convective region $\alpha_1$ in Eq. (7) refers to. If it refers to the albedo of the deep convection cores, then the albedo can change very little because the cloud particle content and optical thickness are already high. If the convective region refers to the region comprising both the convection cores and the anvil clouds, then the albedo of this convective region might decrease with increasing SST and the gradient of SST due to the area response as suggested by Lindzen (1997). In Lindzen et al. (2001), the fractional cover of high-level clouds due to the detrainment of deep convective clouds decreases with increasing SST. Recently, Wielicki et al. (2002) reported that the satellite-inferred OLR in the Tropics increases during the past decade. They suggested that this increase of OLR could not be accounted for by the change in clear-sky radiation and was due to a decrease in clouds. Results from those studies imply that the mean albedo in the convective region of the HMF model might not necessarily increase

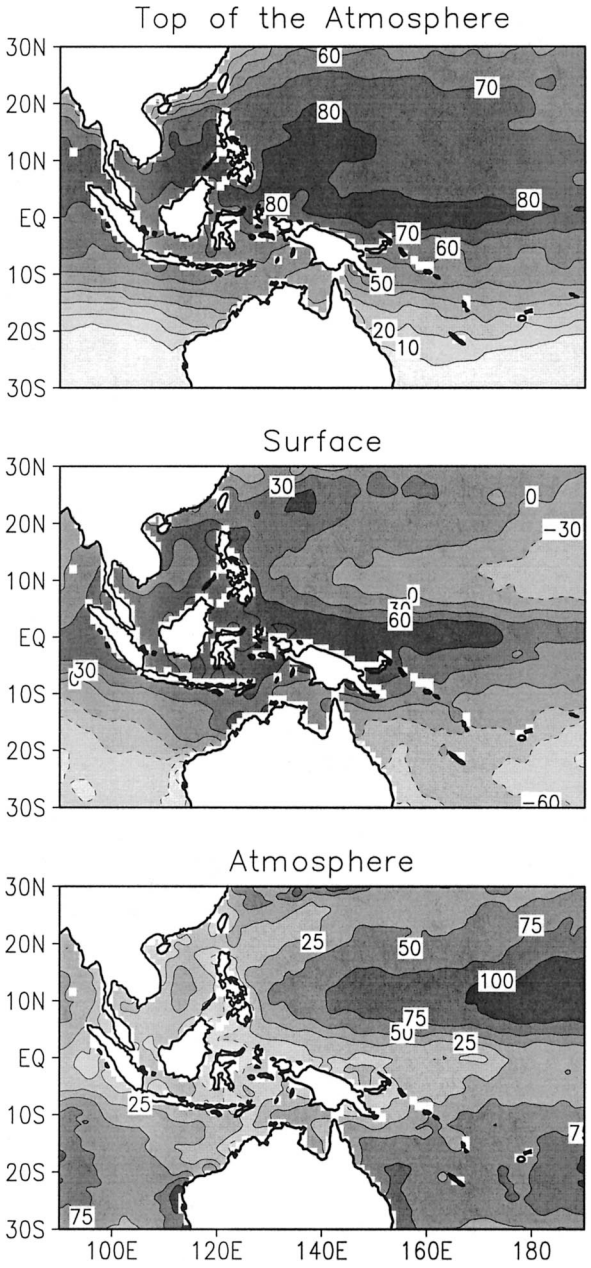


FIG. 4. Net downward fluxes at the TOA and the surface, and the heating of the atmosphere averaged over the period Jan–Aug 1998 (units are W $m^{-2}$).

with increasing $T_1$ and $\omega_1$. Furthermore, those studies also imply that the change in high-level cloud cover could have a large impact on the LW radiation and, hence, climate. This LW impact was essentially ignored by HMF.

Finally, Eqs. (1) and (2) are incorrect. The terms involving the rate of SST change are put there for the purpose of obtaining equilibrium solutions by time integration. For equilibrium solutions, the $R$ terms balance the $M$ terms as shown in Eq. (3). If the mass flux $M$ is

defined only for the atmosphere, then Eqs. (1) and (2) are correct only if the net surface heat flux is negligible in both the convective and nonconvective regions. In this case the net radiative heating of the earth–atmosphere system $R$ is the same as the net heating of the atmosphere. Although the net surface heating has been found to be small in the Pacific warm pool during the Northern Hemispheric winter (Chou et al. 2000), it is not generally so in other tropical regions and seasons. Otherwise the heat fluxes at the sea surface in the Tropics would not be an issue in all long-term climate studies. Figure 4 shows the net downward radiation at the top of the atmosphere, the net surface heating, and the net atmospheric heating in the region (30°S–30°N, 100°E–170°W) during January–August 1998. The TOA net radiation is taken from the Tropical Rainfall Measuring Mission (TRMM) Clouds and the Earth's Radiant Energy System (CERES) archive (Wielicki et al. 1996). The radiation component of the net surface heating is inferred from Japan's Geostationary Meteorological Satellite radiance measurements (Chou et al. 2001). Whereas the surface turbulent heat fluxes are derived using the NCEP SST analysis and the Special Sensor Microwave Imager (SSM/I) precipitable water and wind retrievals (Chou et al. 1997). The atmospheric heating is the difference between the TOA radiation and the surface heating. It can be seen that the net surface heating has a significant spatial variation, ranging approximately from $-60$ to $+60$ W m$^{-2}$. As a result, the net heating of the atmosphere has little resemblance to the TOA radiation.

On the other hand, if the mass flux $M$ is defined as the total mass transport in both the atmosphere and the ocean, then $\omega$ can no longer be the vertical pressure velocity of air. In this case, Eq. (7) and all discussions of $\omega$ in HMF become irrelevant.

*Acknowledgments.* The work of M.-D. Chou was supported by the Radiation Science Program, NASA Office of Earth Science. The efforts of R. S. Lindzen were supported by Grant DE-FG02-01ER63257 from the Department of Energy.

REFERENCES

Barkstrom, B. R., 1984: The Earth Radiation Budget Experiment (ERBE). *Bull. Amer. Meteor. Soc.,* **65,** 1170–1185.

Chou, M.-D., 1994: Radiation budgets in the western tropical Pacific. *J. Climate,* **7,** 1958–1971.

——, P.-K. Chan, and M. M.-H. Yan, 2001: A sea surface radiation data set for climate applications in the tropical western Pacific and South China Sea. *J. Geophys. Res.,* **106,** 7219–7228.

Chou, S.-H., C.-L. Shie, R. M. Atlas, and J. Ardizzone, 1997: Air–sea fluxes retrieved from Special Sensor Microwave Imager data. *J. Geophys. Res.,* **102,** 12 705–12 726.

——, W. Zhao, and M.-D. Chou, 2000: Surface heat budgets and sea surface temperature in the Pacific warm pool during TOGA COARE. *J. Climate,* **13,** 634–649.

Hartmann, D. L., L. A. Moy, and Q. Fu, 2001: Tropical convection and energy balance at the top of the atmosphere. *J. Climate,* **14,** 4495–4511.

Kiehl, J. T., 1994: On the observed near cancellation between longwave and shortwave cloud forcing in tropical regions. *J. Climate,* **7,** 559–565.

Lindzen, R. S., 1997: Can increasing atmospheric $CO_2$ affect global climate? *Proc. Natl. Acad. Sci. USA,* **94,** 8335–8342.

——, M.-D. Chou, and A. Y. Hou, 2001: Does the earth have an adaptive infrared iris? *Bull. Amer. Meteor. Soc.,* **82,** 417–432.

Ramanathan, V., and W. Collins, 1991: Thermodynamic regulation of ocean warming by cirrus clouds deduced from observations of the 1987 El Niño. *Nature,* **351,** 27–32.

Reynolds, R. W., and T. M. Smith, 1994: Improved global sea surface temperature analyses. *J. Climate,* **7,** 929–948.

Rossow, W. B., and R. A. Schiffer, 1991: ISCCP cloud data products. *Bull. Amer. Meteor. Soc.,* **72,** 2–20.

Wielicki, B. A., B. R. Barkstrom, E. F. Harrison, R. B. Lee III, G. L. Smith, and J. E. Cooper, 1996: Clouds and the Earth's Radiant Energy System (CERES): An earth observing system experiment. *Bull. Amer. Meteor. Soc.,* **77,** 853–868.

——, and Coauthors, 2002: Evidence for large decadal variability in the tropical mean radiative energy budget. *Science,* **295,** 841–844.